

# Accounting for the kinetics in order parameter analysis: lessons from theoretical models and a disordered peptide

Ganna Berezovska, Diego Prada-Gracia, Stefano Mostarda, and Francesco Rao\*

Freiburg Institute for Advanced Studies, School of Soft Matter Research, Freiburg im Breisgau, Germany.

(Dated: June 3, 2022)

Molecular simulations as well as single molecule experiments have been widely analyzed in terms of order parameters, the latter representing candidate probes for the relevant degrees of freedom. Notwithstanding this approach is very intuitive, mounting evidence showed that such description is not accurate, leading to ambiguous definitions of states and wrong kinetics. To overcome these limitations a framework making use of order parameter fluctuations in conjunction with complex network analysis is investigated. Derived from recent advances in the analysis of single molecule time traces, this approach takes into account of the fluctuations around each time point to distinguish between states that have similar values of the order parameter but different dynamics. Snapshots with similar fluctuations are used as nodes of a transition network, the clusterization of which into states provides accurate Markov-State-Models of the system under study. Application of the methodology to theoretical models with a noisy order parameter as well as the dynamics of a disordered peptide illustrates the possibility to build accurate descriptions of molecular processes on the sole basis of order parameter time series without using any supplementary information.

## INTRODUCTION

Order parameters are conventionally used for the characterization of complex molecular processes [1, 2]. Inter-atomic distances or a combination of them are common choices, providing an intuitive description in terms of free-energy projections [3–7]. Unfortunately, it has been repeatedly found that reduced descriptions based on order parameters are often inaccurate [8–13]. The origin of the failure is due to overlaps in the order parameter distribution, i.e., configurations with different properties corresponding to the same value of the coordinate, making the discrimination between states ambiguous [10, 12]. From the point of view of the dynamics, spurious recrossings at the borders result in lower free-energy barriers and artificially faster kinetics [14].

To improve on this situation, a new arsenal of tools emerged making use of complex networks and the theory of stochastic processes. Configuration-space-networks, referred as Markov-State-Models when the Markov property is satisfied, provide high resolution free-energy landscapes of complex molecular processes [8, 9, 15–19]. The main idea behind this approach is to map the molecular dynamics onto a transition network. Nodes and links represent sampled system configurations (*microstates*) and the transitions between them as observed in the molecular dynamics, respectively. The resulting transition network stores the entire kinetical information in the form of link weights and node connectivity, providing a compact representation of the molecular trajectory. Within this approach, free-energy representations are obtained in a more universal way without using arbitrarily projections on order parameters. Both thermodynamics and kinetics come from the analysis of the transition network with methods like network clusterization algorithms [15, 18, 20], network flow analysis [9, 19, 21] and spectral

methods [16, 17].

Besides the advantages, a general strategy towards microstates building is still missing, making the initial mapping of the molecular trajectory onto a network non-trivial. Even for the well-studied case of structured peptides and the folding of small proteins, there is no consensus on the best practice [19, 22]. Moreover, a broad set of problems including molecular association [23, 24], the analysis of intrinsically disordered proteins [25, 26] and liquids [27, 28] are very hard to tackle with the current methodology. As shown for the case of water, *ad-hoc* strategies are needed [29–31]. Ironically, many of these processes can be qualitatively described by the analysis of conventional order parameters.

In this work, an effort is made to reconcile the intuitive aspect of order parameters with the predictive power of transition networks, overcoming some of the limitations of both methodologies. The strategy couples a recently developed framework for the analysis of single molecule traces [32–34] using network clusterization techniques in order to obtain accurate kinetic models from conventional order parameter time series. Applications to theoretical models and molecular dynamics simulations of a disordered peptide are presented. Our results suggest a general approach to analyze molecular processes with high accuracy on the sole basis of conventional order parameter time series.

## THEORY

### Configuration-space networks from conventional order parameters

*General motivation.* Order parameters allow for intuitive descriptions of molecular processes. Unfortunately,

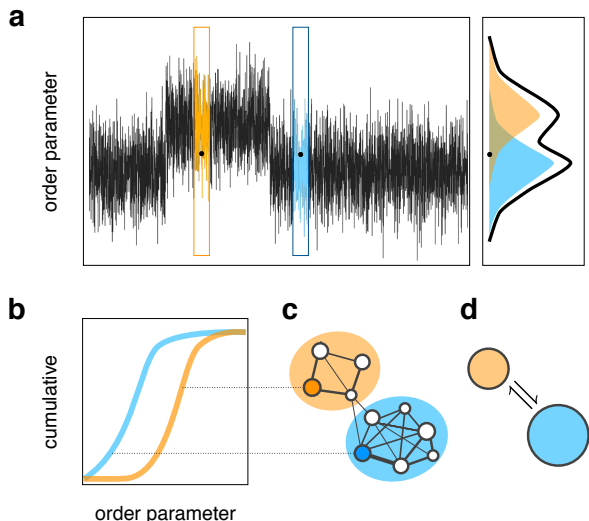


FIG. 1. Local-fluctuations order parameter analysis. (a) The time series of an order parameter and its distribution (black lines). Two snapshots with the same value of the order parameter but belonging to different states are characterized by distinct local distributions (orange and light blue, respectively). (b) A Kolmogorov-Smirnov test evaluates the similarity of the cumulative of the two distributions. Snapshots with similar distributions belong to the same *microstate*. (c) Microstates and the transitions between them represent nodes and links of a configuration-space-network, respectively. Network clusterization techniques allow the lumping of kinetically homogeneous regions of the network into states (orange and light blue areas) (d) States are used to build a reduced Markov-State-Model of the original molecular process (see the Theory section for further details).

such descriptions can be highly inaccurate due to the presence of *overlaps*, i.e., configurations with different properties corresponding to the same value of the order parameter [10, 12]. An important improvement in this respect was the introduction of configuration-space-networks, providing accurate and concise descriptions of the system kinetics and thermodynamics [8, 9, 15–19]. Their application however is still limited, lacking a general way to build the transition network.

To overcome this impasse, a potential strategy makes use of a recently introduced framework for the analysis of single molecule experiments [32–34]. Local fluctuations of a given coordinate bring relevant information on the underlying free-energy surface. That is, two points with similar values of the coordinate but belonging to different states are characterized by distinct local distributions (see orange and blue areas in Fig. 1a). In order to characterize the molecular process, this information can be used in different ways, going from the concept of state “candidate” based on escape times [32, 34] to cut-based free-energy profiles [33]. The latter approach proposed a way to build the system microstates based on the local

fluctuations of an arbitrary inter-atomic distance, showing that the folding barrier and native state population of a small protein are correctly recovered. On the other hand, the limited information contained in a single distance made the full reconstruction of the unfolded state hard.

Here, local fluctuations are exploited towards a better characterization of order parameter time series, overcoming the problems raised by the presence of overlaps. The proposed protocol works as follows: (i) based on the time series of the order parameter a set of microstates is constructed; (ii) the resulting configuration-space-network is built; (iii) the presence of states is found by performing a network clusterization algorithm; (iv) a reduced kinetic model is built based on the found states. These four steps are described in detail below.

*Microstate building.* The microstates accounting for the local fluctuations of the order parameter were built as suggested in Ref. [33]. As such, each time point of the trajectory  $t_i$  was associated with a corresponding time window  $[t_i - \tau/2, t_i + \tau/2]$ . Two time points were considered to be *similar* if they have comparable distributions of the order parameter. Snapshot similarity,  $D$ , was estimated by comparing the cumulative of the two distributions via a Kolmogorov-Smirnov test [35] which checks whether two samples belong to the same distribution or not (Fig. 1b).  $D$  was defined as the maximum difference of the two cumulative distributions. Two samples belong to the same distribution, and thus to the same microstate, if the condition  $D \leq \zeta \sqrt{2/\tau}$  was fulfilled. The acceptance cutoff  $\zeta$  corresponds to a certain confidence level. Being  $\tau$  and  $\zeta$  related, we fixed the latter value to 0.5 and let  $\tau$  vary. Comparisons were made along the trajectory using the leader algorithm in a way that each time point was associated to a microstate at the end of the procedure [33, 36].

*The configuration-space-network.* The resulting time series of microstates was mapped onto a configuration-space-network (Fig. 1c). Microstates represent network nodes and a link between them exists if they were successively visited along the molecular trajectory. For each link detailed balance was imposed by making an average of the number of transitions in both directions.

*Network clusterization.* A clusterization algorithm was applied for the analysis of the configuration-space-network in order to detect the presence of states. In fact, free-energy basins are represented as densely connected regions of the configuration-space-network [15]. It was shown [15, 18] that those regions can be automatically detected by using the Markov-Clustering-Algorithm (MCL) for network clusterization [37]. This approach is based on the evolution of random walkers on the network, resulting in a kinetically accurate network splitting. Hence, dynamical interconversions within a cluster are faster than transitions to other regions of the network. Being separated by barriers, network clusters represent free-energy

basins (i.e., the *states*) of the system (orange and blue areas in Fig. 1c). A parameter  $p > 1$  tunes the granularity of the clusterization. Larger values of the parameter (e.g.  $p > 1.5$ ) result in an increased number of clusters while the most relevant states (i.e. separated by the highest barriers) are already detected with  $p$  between 1.2 and 1.4 [15, 18].

*Reduced kinetic model.* The most populated clusters were used as states of a reduced Markov-State-Model. Transition probabilities were estimated from the original transition network by summing up all the links connecting any two states (orange and blue areas in Fig. 1c-d). It is worth noting that while this reduced kinetic model satisfies the Markov property [19], this is not generally the case for the starting transition network. (This property is in any case not needed when it comes to network clusterization [15, 18].) The accuracy of the kinetic model was estimated with the use of first-passage-time distributions.

## METHODS

### Two-state model

A stochastic two-state model with transition probability  $p_{ij} = 0.01$  was built. The latter probability completely defines the kinetics of the model. The time evolution was monitored by an artificially defined order parameter  $Q$  in a way that  $Q$  cannot distinguish between the two states unambiguously (see dark blue line in Fig. 2a for a sample time series).  $Q$  was associated to an energy function  $U_1 = \alpha Q^2$  and  $U_2 = \alpha(Q - 1)^2$  for the two states, respectively. As such, the first and second states preferentially visit different values of the order parameter. Within each state, the time evolution of  $Q$  was obtained by a conventional Metropolis criterion  $\min[1, \exp(-\beta\Delta U)]$  with  $\beta$  regulating the amount of fluctuations. Choosing  $\alpha = 16$ , values of  $\beta$  close to 1 suppress fluctuations while smaller values enhance them (most of the treatment below was done for the case of large fluctuations with  $\beta = 0.3$ ). This model was used to generate order parameter time series of  $10^5$  steps.

### Molecular dynamics simulations

Simulations of the (Gly-Ser)<sub>2</sub> flexible linker peptide were performed using the all-atom CHARMM force-field version 27 [38, 39] as implemented in the program ACEMD [40]. All calculations were done on NVIDIA GTX680 graphics cards. The system was solvated into a box containing 1560 TIP3P waters. After equilibration, the molecular dynamics was run for  $1\mu\text{s}$  in the NVT ensemble at 300K, using the Langevin algorithm. An integration time step of 4 fs was used by rescaling the hydro-

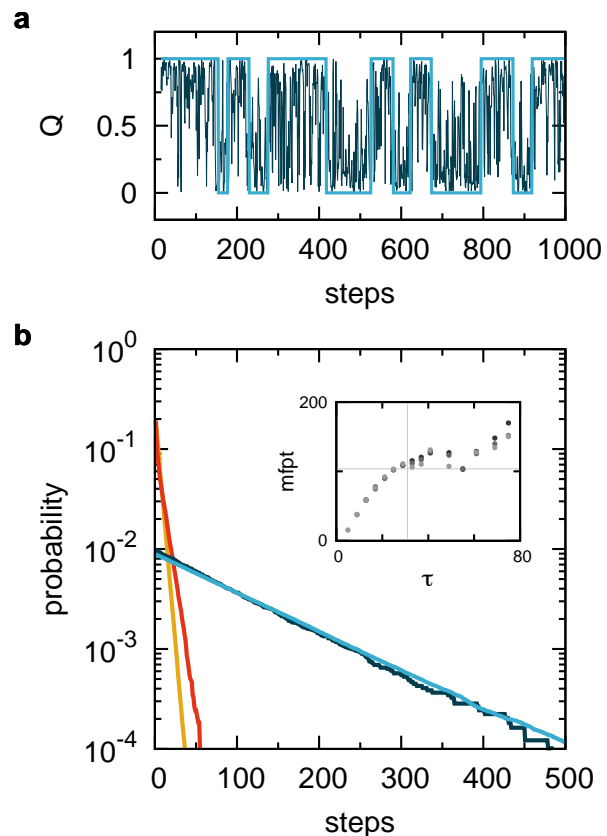


FIG. 2. Theoretical two-state model. (a) The time series of the order parameter  $Q$  and the corresponding states obtained with the local-fluctuations analysis are shown in dark and light blue, respectively; (b) first-passage time distributions obtained by different analysis techniques. The distribution corresponding to the original two-state model is shown in dark blue. Distributions obtained from the local-fluctuations reduced kinetic model, a naive two-state model and along the original time series using  $Q = 0.5$  as state separator are shown in light blue, yellow and red lines, respectively. The dependence of the mean-first-passage-time (mfpt) with the time window size  $\tau$  is shown in the inset (MCL  $p$  parameter of 1.3 and 1.4 for gray and dark gray points, respectively). The correct value of the mfpt and the time window value chosen for the analysis are shown as horizontal and vertical lines, respectively.

gen mass to 4 amu together with mass repartitioning [41]. The radius of gyration was calculated with the program WORDOM [36, 42], neglecting all peptide hydrogens.

## RESULTS

### A two-state process with large fluctuations

The protocol described in the Theory section was applied to the time series of a generic order parameter  $Q$  with an underlying two-state dynamics. This model

served as a benchmark for the proposed network approach since the underlying kinetics is known by construction. The amount of fluctuations of the order parameter  $Q$  is controlled by a parameter  $\beta$  (see Methods). To characterize the two-state behavior directly from the time series a *naive* strategy would take the distribution of  $Q$ , looking for the minimum separating the two states. The value of  $Q$  at the minimum, 0.5 in this case, defines the separator between the states. If the fluctuations around the separator are small,  $Q$  is a good order parameter in the sense that the number of crossings of the separator represents a good estimate of the barrier between the two states. This approach is valid for the case of small fluctuations but breaks down as soon as the overlap between the states increases (i.e. large fluctuations). In the latter case, most of the contributions to the separator are coming from re-crossings: transitions passing the separator coming back very quickly to the initial state without reaching the end state. The origin of recrossings is mostly due to a sub-optimal choice of the order parameter rather than to a real physical property.

The time series of  $Q$  for the case of large fluctuations ( $\beta = 0.3$ ) was characterized with different approaches. A particular stringent test consists in the calculation of the first-passage-time (fpt) distribution to one of the two states. The correct distribution is shown as a dark blue line in Fig. 2b (mean-fpt of 103.85 steps). This distribution is greatly influenced by the definition of the target state. If the latter is correctly defined, the resulting distribution overlap with the one calculated from the original two-state model. When the target state was chosen as  $Q < 0.5$ , a fpt distribution calculated along the trajectory resulted in a much faster kinetics (red line, Fig. 2b). With a mfpt of 7.56 steps, the kinetics obtained by this analysis was one order of magnitude faster with respect to the input model.

A better description was obtained by analyzing the time series in terms of local-fluctuations and Markov-State-Models. The microstates were obtained by the protocol described in the Theory section (Fig. 1). Clusterization of the resulting transition network resulted in the detection of two states. Being based on the order parameter fluctuations, these states are not strictly separated in terms of  $Q$  as shown by their time series (light blue, Fig. 2a). These two states were used to build a new Markov-State-Model with transition probabilities estimated from the original transition network (see Methods). In this case, the fpt distribution was estimated by generating a new time series of  $10^6$  steps from this model. Strikingly, the fpt distribution calculated on this new trajectory perfectly overlapped to the one generated by the original two-state model as shown by the light blue line of Fig. 2b. Using a time window  $\tau = 30$ , the resulting mfpt is of about 114.58 steps, very close to the correct value of 103.85. This is not the case when a two-state model was built by estimating the transition probabil-

ity from the number of times the separator  $Q = 0.5$  was crossed. As expected, the fpt distribution calculated on the time series generated by this model leads to very poor results because the inter-state separator is dominated by recrossings (mfpt=5.2, yellow line, Fig. 2b).

It is important to note that the two kinetic models presented here (corresponding to the light blue and yellow lines) were built using the same starting information, i.e. the time series of the order parameter  $Q$ . Consequently, the improvement obtained by the local-fluctuations analysis is purely due to the different strategy applied rather than the use of supplementary information.

It is important to note that the predictions may depend on the choice of the time window  $\tau$  (see Theory). Caffisch and coworkers found a large range of validity for this parameter [33]. For the present two-state model, the time window range was evaluated against the mfpt to reach the target state (inset of Fig. 2b). For small time windows the value of the mfpt was smaller with respect to the correct one (horizontal line). This is due to the incorrect detection of states where large fluctuations were detected as real transitions. As the value of  $\tau$  was increased, the mfpt first converged to values close to the theoretical one ( $30 < \tau < 60$ ) and then increased again. It was found that when the time window was too large, some transitions were missed, resulting in an overall slower kinetics. Consequently, the behavior of the mfpt as a function of  $\tau$  suggests a reasonable way to choose the time window as the location of the first slope change ( $\tau = 30$ , vertical line), just before the convergence region. Essentially identical results were found for the MCL parameter  $p = 1.3 - 1.4$  (inset of Fig. 2b).

### Multi-state dynamics of a disordered peptide

GlySer peptides have been used in experiments for quite some time as flexible linkers [43, 44]. Short stretches of this peptide are interesting from a theoretical point of view because they are computationally tractable, presenting non-trivial conformational disorder [20, 45, 46]. In this section the local-fluctuations analysis is applied to the dynamics of a (Gly-Ser)<sub>2</sub> peptide. To this aim, a long molecular dynamics simulation of 1  $\mu$ s was performed. It has been shown [46] that the radius of gyration  $R_g$  qualitatively describes the conformational disorder of this peptide, suggesting the presence of multiple states. A time series stretch and the distribution of the  $R_g$  are shown as a dark blue line and a gray area in panel a and b of Fig. 3, respectively.

Application of the local-fluctuations analysis on the  $R_g$  time series revealed the presence of five major states ( $\tau = 300$  ps and  $p = 1.3$ ; these two values were chosen following the mfpt based strategy of the previous section). Fig. 3b shows the  $R_g$  distribution of the five states (colored lines). Interestingly, the five distributions are

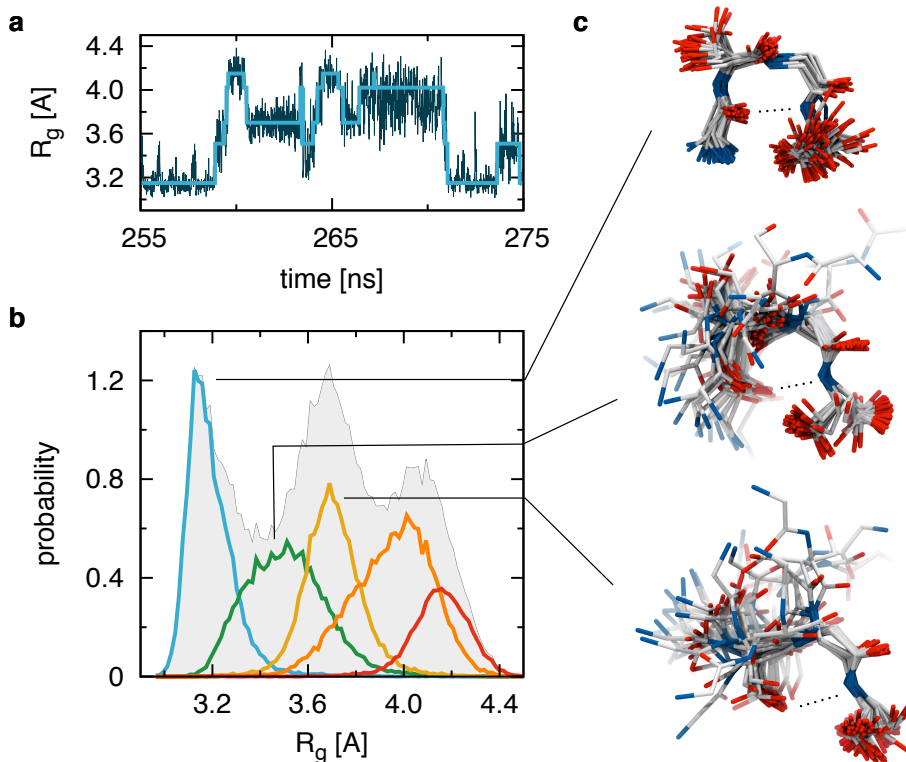


FIG. 3. The  $(\text{Gly-Ser})_2$  peptide. (a) A time series stretch of the radius of gyration ( $R_g$ , dark blue) and of the detected states after the local-fluctuations analysis (light blue); (b) Distribution of the radius of gyration. The distributions from the entire trajectory and for the five most populated states are shown as a gray area and colored lines, respectively. (c) Structural characterization of the three most compact states. For each of them, 50 random snapshots were overimposed.

largely overlapping making their detection impossible by simply looking at the total distribution. In fact, the total distribution suggested no more than three states as indicated by the number of peaks (gray area in Fig. 3b). Interestingly, the presence of the five states was already apparent in the raw  $R_g$  time series (dark blue line, Fig. 3a). Those states became hidden in the total distribution due to the large fluctuations, reiterating the idea that using free-energy projections for the characterization of molecular processes can be ambiguous.

From a structural point of view, all five states are well characterized. A molecular representation of the three most compact states is shown in Fig. 3c. The most compact one, coded in light blue in Fig. 3b, corresponds to a loop-like structure typically found in  $\beta$ -strands turns. This structure is stabilized by a hydrogen bond between the first backbone oxygen  $O_1$  and nitrogen  $N_4$ . This conformation has a population of around 23% and  $R_g \approx 3.1$  Å. The second state has a population of 22% and  $R_g \approx 3.5$  Å (green curve in Fig. 3b). Its topology is very similar to the turn-like structure but it is more disordered due to the formation of a non optimal backbone hydrogen bond. The third state instead is stabilized by the interaction of the side chain oxygen of  $\text{SER}_2$  with the backbone nitrogen  $N_4$  (population of 20%

and  $R_g \approx 3.7$  Å, yellow curve in Fig. 3b). In this structure, the side chain substitutes the backbone oxygen as a partner in the hydrogen bond, acting as a trap towards further compaction. Finally, the last two states (orange and red curves in Fig. 3b) are rather unstructured, providing similar realizations of almost completely extended conformations.

To check whether the kinetics of the Markov-State-Model built on top of the five detected states reflected the same dynamics of the original trajectory, a fpt analysis was performed (Fig. 4). In light blue, the fpt distribution to the compact state was calculated on a trajectory originated from the Markov-State-Model. To compare it with the molecular dynamics simulation, the fpt to conformations with  $R_g = 3.16 \pm 0.01$  (the top of the first peak in the  $R_g$  distribution) was calculated along the original molecular dynamics trajectory (dark blue line in Fig. 4). This represents a good estimate of the fpt to the compact state at long times. Strikingly, the two curves nicely overlapped. An exponential fit of the data, i.e.  $\sim \exp(-t/t_r)$ , showed a relaxation time of 6.5 ns in both cases.

The fpt distribution calculated along the original trajectory using as target state all conformations with  $R_g < 3.4$  (this is the value of the minimum of the  $R_g$  dis-

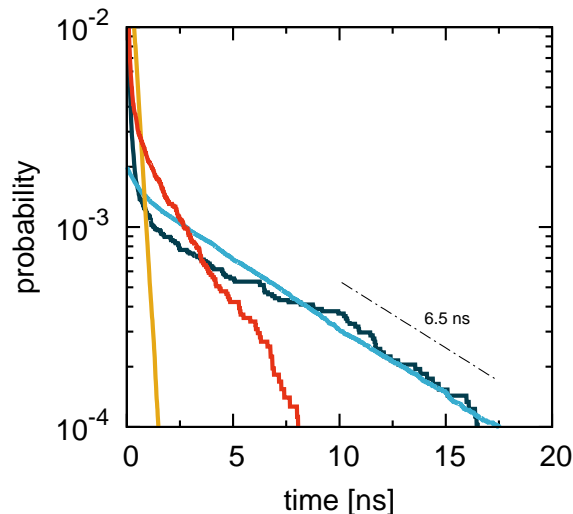


FIG. 4. The  $(\text{Gly-Ser})_2$  first-passage-time distribution. Distributions obtained from the local-fluctuations analysis, a naive two-state model and along the original time series are shown in light blue, yellow and red, respectively. For the latter two cases the target of the relaxation was  $R_g < 3.4$ . The relaxation kinetics to the compact state defined as the conformations belonging to the first peak of the  $R_g$  ( $R_g = 3.16 \pm 0.01$ , see Fig. 3b) is shown in dark blue.

tribution) provided a much faster kinetics (red line in Fig. 4). However, processes involving barrier crossings are expected to have the same relaxation kinetics when either the whole state is selected as a target or just the most probable conformation of the state (i.e. conformations at the peak of the order parameter distribution) [19]. Consequently, the disagreement between the fpt distribution to  $R_g < 3.4$  and to a more stringent target (i.e.  $R_g = 3.16 \pm 0.01$ ), provides strong evidence that the correct estimation of the kinetics cannot be obtained directly from the  $R_g$  distribution due to the presence of recrossings. As expected, this becomes even worse when the Markov-State-Model is built directly from the  $R_g$  distribution, i.e. by choosing as states the portions of the distribution separated by minima and as transition probabilities the number of times the minima were crossed (yellow line in Fig. 4).

## DISCUSSION

Nowadays, molecular dynamics simulations easily produce tera scale of data. As such, an important bottleneck in the understanding of molecular processes is in the analysis rather than the data generation per se.

In this work, a strategy for the analysis of conventional order parameters time series that is kinetics compliant was investigated. Our results provided strong evidence that the coupling of order parameter fluctuations with

complex network analysis represents a powerful approach to deconvolute crowded order parameter distributions of molecular systems. This procedure allows the construction of kinetically accurate Markov-State-Models in a natural and intuitive way, largely overcoming the problems raised by conventional order parameter analysis. Moreover, a wide range of experimentally generated time traces coming from FRET or optical tweezers, can be readily tackled by this methodology.

Taking into account the fluctuations within a time-window  $\tau$ , the approach is able to distinguish between snapshots belonging to different states but having the same value of the order parameter. Towards an accurate characterization of the kinetics the value of  $\tau$  needs to be chosen appropriately. We proposed to estimate it on the basis of a mean-first-passage-times analysis. Very similar in spirit to what Caffisch and collaborators proposed in their work [33], this procedure is more suitable to our network clusterization approach.

Finally, it is worth mentioning that instead of looking at better ways to analyze conventional order parameters time series, some groups focused their attention on the development of optimal reaction coordinates [47–49]. These abstract coordinates aim to correctly characterize the molecular kinetics. Among them, one method based on cut-based free-energy profiles seems very promising [49]. In this approach, the coefficients of a linear combination of physical distances are optimized against the cut-based free-energy profile. At the end of the process, the combination which maximizes the barrier height with respect to a target state provides the optimal reaction coordinate. A fundamental difference between this method and the local-fluctuations analysis is that the latter requires the time evolution of a single (non-optimal) coordinate while the optimization procedure makes use of a very large number of physical distances (usually around thousands [14, 49, 50]) to perform properly.

\* francesco.rao@frias.uni-freiburg.de

- [1] R. Du, V. Pande, A. Grosberg, T. Tanaka, and E. Shakhnovich, *J. Chem. Phys.* **108**, 334 (1998).
- [2] S. Benkovic, G. Hammes, and S. Hammes-Schiffer, *Biochem.* **47**, 3317 (2008).
- [3] T. Lazaridis and M. Karplus, *Science* **278**, 1928 (1997).
- [4] A. Dinner, A. Sali, L. Smith, C. Dobson, and M. Karplus, *Tr. Biochem. Sci.* **25**, 331 (2000).
- [5] R. Zhou, B. Berne, and R. Germain, *Proc. Nat. Acad. Sci. USA* **98**, 14931 (2001).
- [6] F. Rao and A. Caffisch, *J. Chem. Phys.* **119**, 4035 (2003).
- [7] M. Cecchini, F. Rao, M. Seeber, A. Caffisch, *et al.*, *J. Chem. Phys.* **121**, 10748 (2004).
- [8] F. Rao and A. Caffisch, *J. Mol. Biol.* **342**, 299 (2004).
- [9] S. V. Krivov and M. Karplus, *Proc. Natl. Acad. Sci. USA* **101**, 14766 (2004).
- [10] F. Rao, G. Settanni, E. Guarnera, and A. Caffisch, *J.*

- Chem. Phys. **122**, 184901 (2005).
- [11] R. Hegger, A. Altis, P. Nguyen, and G. Stock, Phys. Rev. Lett. **98**, 28102 (2007).
- [12] S. Muff and A. Caffisch, Proteins **70**, 1185 (2008).
- [13] G. Maisuradze, A. Liwo, and H. Scheraga, Phys. Rev. Lett. **102**, 238102 (2009).
- [14] S. Krivov, J. Phys. Chem. B **115**, 12315 (2011).
- [15] D. Gfeller, P. De Los Rios, A. Caffisch, and F. Rao, Proc. Natl. Acad. Sci. USA **104**, 1817 (2007).
- [16] F. Noé, I. Horenko, C. Schütte, and J. C. Smith, J. Chem. Phys. **126**, 155102+ (2007).
- [17] J. D. Chodera, N. Singhal, V. S. Pande, K. A. Dill, and W. C. Swope, J. Chem. Phys. **126**, 155101+ (2007).
- [18] D. Prada-Gracia, J. Gómez-Gardeñes, P. Echenique, and F. Falo, PLoS Comp. Biol. **5**, e1000415+ (2009).
- [19] F. Rao, S. Garrett-Roe, and P. Hamm, J. Phys. Chem. B **114**, 15598 (2010).
- [20] F. Rao, J. Phys. Chem. Lett. **1**, 1580 (2010).
- [21] S. V. Krivov and M. Karplus, J. Phys. Chem. B **110**, 12689 (2006).
- [22] E. Hua-Mei Kellogg, O. Lange, and B. D., J. Phys. Chem. B (2012), 10.1021/jp3044303.
- [23] I. Buch, T. Giorgino, and G. De Fabritiis, Proc. Nat. Acad. Sci. USA **108**, 10184 (2011).
- [24] D. Huang and A. Caffisch, PLoS Comp. Biol. **7**, e1002002 (2011).
- [25] V. Uversky, C. Oldfield, and A. Dunker, Annu. Rev. Biophys. **37**, 215 (2008).
- [26] M. Knott and R. Best, PLoS Comp. Biol. **8**, e1002605 (2012).
- [27] J. Errington and P. DeBenedetti, Nature **409**, 318 (2001).
- [28] T. Yan, C. Burnham, M. Del Pópolo, and G. Voth, J. Phys. Chem. B **108**, 11877 (2004).
- [29] F. Rao, S. Garrett-Roe, and P. Hamm, J. Phys. Chem. B **114**, 15598 (2010).
- [30] S. Garrett-Roe, F. Perakis, F. Rao, and P. Hamm, J. Phys. Chem. B **115**, 6976 (2011).
- [31] D. Prada-Gracia and F. Rao, arXiv:1207.6953 (2012).
- [32] A. Baba and T. Komatsuzaki, Proc. Natl. Acad. Sci. USA **104**, 19297 (2007).
- [33] P. Schuetz, R. Wuttke, B. Schuler, and A. Caffisch, J. Phys. Chem. B **114**, 15227 (2010).
- [34] A. Baba and T. Komatsuzaki, Phys. Chem. Chem. Phys. **13**, 1395 (2011).
- [35] N. V. Smirnov, Mat. Sb. **6**, 3 (1939).
- [36] M. Seeber, M. Cecchini, F. Rao, G. Settanni, and A. Caffisch, Bioinf. **23**, 2625 (2007).
- [37] A. J. Enright, S. Van Dongen, and C. A. Ouzounis, Nucl. Ac. Res. **30**, 1575 (2002).
- [38] B. Brooks, R. Bruccoleri, B. Olafson, S. Swaminathan, M. Karplus, *et al.*, J. Comp. Chem. **4**, 187 (1983).
- [39] B. Brooks, C. Brooks III, A. Mackerell Jr, L. Nilsson, R. Petrella, B. Roux, Y. Won, G. Archontis, C. Bartels, S. Boresch, *et al.*, J. Comp. Chem. **30**, 1545 (2009).
- [40] M. Harvey, G. Giupponi, and G. Fabritiis, J. Chem. Th. Comp. **5**, 1632 (2009).
- [41] K. A. Feenstra, B. Hess, and H. J. C. Berendsen, J. Comp. Chem. **20**, 786 (1999).
- [42] M. Seeber, A. Felling, F. Raimondi, S. Muff, R. Friedman, F. Rao, A. Caffisch, and F. Fanelli, J. Comp. Chem. **32**, 1183 (2011).
- [43] O. Bieri, J. Wirz, B. Hellrung, M. Schutkowski, M. Drewello, and T. Kiefhaber, Proc. Nat. Acad. Sci. USA **96**, 9597 (1999).
- [44] A. Möglich, K. Joder, and T. Kiefhaber, Proc. Nat. Acad. Sci. **103**, 12394 (2006).
- [45] F. Rao, J. Comp. Chem. **32**, 1113 (2011).
- [46] F. Rao and M. Spichty, J. Comp. Chem. **33**, 475 (2012).
- [47] R. Best and G. Hummer, Proc. Nat. Acad. Sci. USA **102**, 6732 (2005).
- [48] A. Ma and R. Aaron, J. Phys. Chem. B **109**, 6769 (2005).
- [49] S. Krivov, J. Phys. Chem. B **115**, 1138211388 (2011).
- [50] S. Steiner and A. Caffisch, Proteins (2012), 10.1002/prot.24137.